Experimental and Analytical Studies of Lightning Overvoltages in Wind Turbine Generation Systems

K. Yamamoto, T. Noda, S. Yokoyama, A. Ametani

Abstract-- This paper presents the results of the experimental and analytical studies undertaken for the lightning protection of wind turbine generation systems by using a reduced-size wind turbine model. In the analytical studies, the FDTD (Finite Difference Time Domain) method is used. This study focuses on the overvoltages observed at the wavefronts of lightning surges. The lightning strokes on one of the blades and on the nacelle were considered, and the experiments and analyses were carried out by considering the cases of summer and winter lightning. The voltages and currents at various positions on the wind turbine model were considered.

Keywords: wind turbine generation systems, lightning, surge, FDTD method, overvoltages

I. INTRODUCTION

In recent years, the proliferation of wind turbine generation systems has resulted in many accidents caused by natural phenomena such as lightning and typhoons. In particular, this paper focuses on the extensive damage caused by lightning.

In order to achieve good wind conditions, wind turbine generation systems are often constructed on hilly terrain or at the seashore where few tall structures exist in the vicinity; therefore, these structures are often struck by lightning. For promoting wind power generation, lightning-protection methodologies should be established for wind turbine generation systems [1]-[3].

We present the results of experimental and analytical studies for the lightning protection of wind turbine generation systems by using a reduced-size wind turbine model. This study focuses on the overvoltages observed at the wavefronts of lightning surges. Assuming lightning strokes at the tip of a blade and the rear portion of a nacelle, fast-front currents were injected into these points, and the experiments and analyses were carried out by considering the cases of summer and

winter lightning. The voltages at the current-injection points and various voltage differences were measured with different wavefronts of the injected current and different grounding resistances. For the analytical studies based on the measured results, FDTD (Finite Difference Time Domain) method [4] was used.

II. EXPERIMENTAL CONDITIONS

A reduced-size model, as shown in Fig. 1, was used in the experiments. It is a 3/100-scale model of an actual wind turbine generation system that has blades with a length of 25 m and a tower that is 50 m high. The material of the blades is vinyl chloride, and an insulated copper wire with a cross-sectional area of 2 mm^2 is traced on each blade to represent a lightning conductor. The actual tower is tapered; however, the tower of the scale model is of the tubular-type with an outer diameter of 10 cm and a thickness of 3 mm. The nacelle is a metal cube with a side length of 15 cm.

The above mentioned reduced-size model was set up as shown in Fig. 2. Many aluminium plates which have a thickness of 2 mm were embedded in the ground so that the aluminium floor could be considered to be infinite in the time dimension of the measurements. The assumed point of the lightning strokes is the tip of one of the blades, as shown in Fig. 2 (a), or the rear portion of the nacelle, as shown in Fig. 2 (b). In the case of the measurements for summer lightning, the return stroke propagates from the wind turbine generation system to the cloud. Here, the current is injected into the coaxial cable from the pulse generator and is led to the lightning-stroke point. The current is injected into the reduced-size model of a wind turbine generation system through the resistance R_i. While the current propagates on the
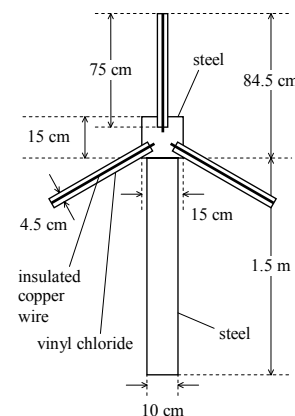
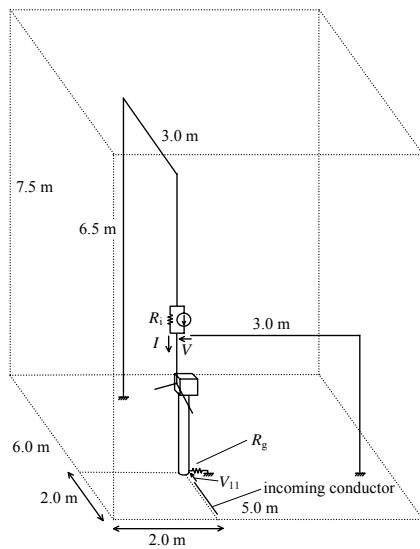Fig. 1.   Reduced-size model of a wind turbine generation system

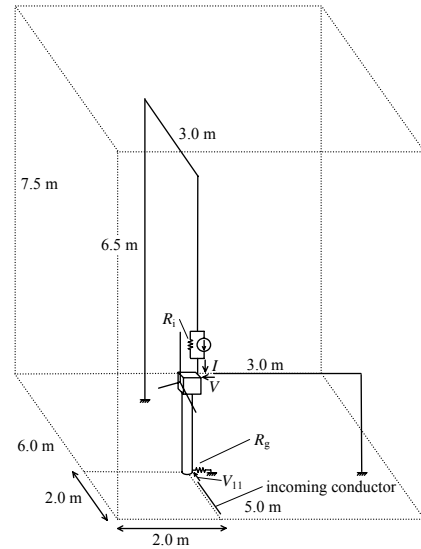(a) Case of summer and winter lightning strokes on one of the blades

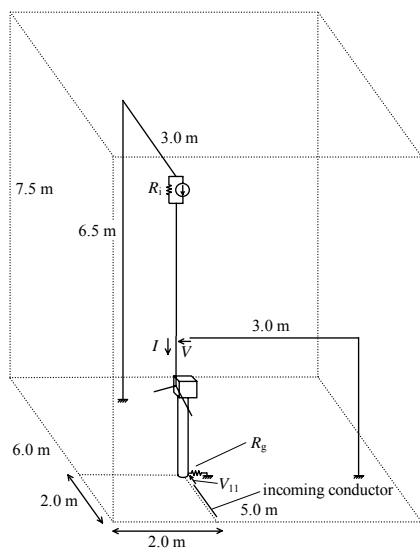(b) Case of summer and winter lightning strokes at the rear portion of the nacelle

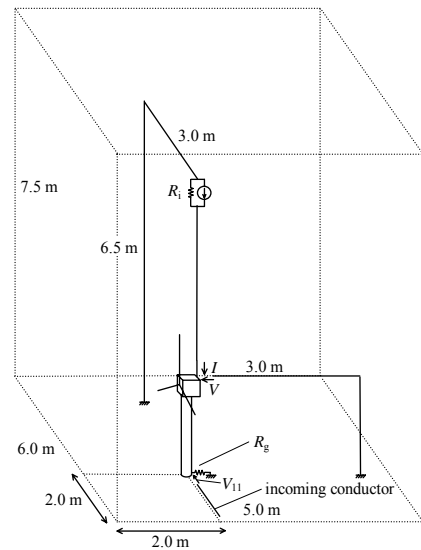Fig. 2. Configuration of experimental setup

(a) Case of a summer lightning stroke on one of the blades

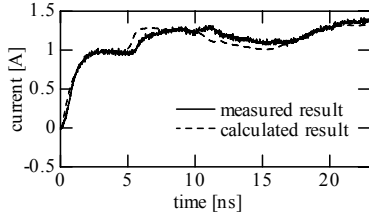(b) Case of a summer lightning stroke at the rear portion of the nacelle

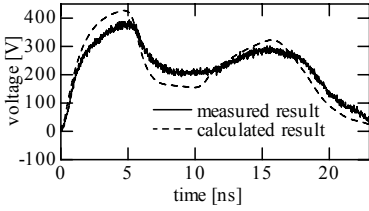(c) Case of a winter lightning stroke on one of the blades

(d) Case of a winter lightning stroke at the rear portion of the nacelle

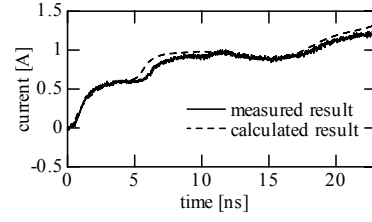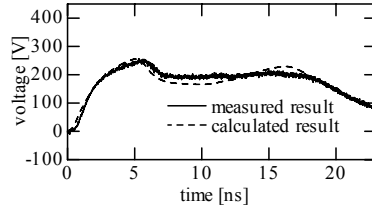Fig. 3. Configuration of FDTD analyses

(a) Current *I*

(b) Voltage *V*

Fig. 4. Current *I* and potential *V* at the lightning-stroke point under the conditions of summer lightning, tip of blade, R_g = 9.4 Ω, and τ = 4 ns

(a) Current *I*

(b) Voltage *V*

Fig. 5. Current *I* and potential *V* at the lightning-stroke point under the conditions of summer lightning, rear portion of a nacelle, R_g = 9.4 Ω, and τ = 4 ns
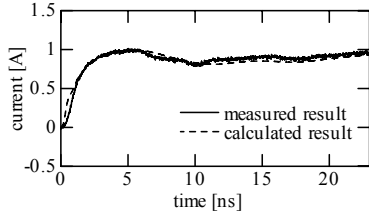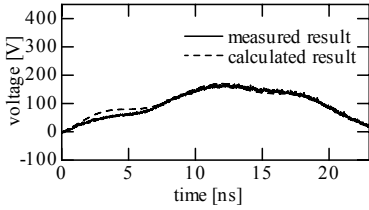

(a) Current *I*

(b) Voltage *V*

Fig. 6. Current *I* and potential *V* at the lightning-stroke point under the conditions of winter lightning, tip of blade, R_g = 9.4 Ω, and τ = 4 ns
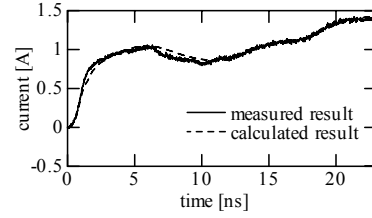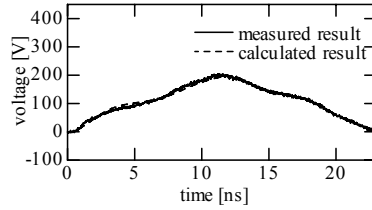

(a) Current *I*

(b) Voltage *V*

Fig. 7. Current *I* and potential *V* at the lightning-stroke point under the conditions of winter lightning, rear portion of a nacelle, R_g = 9.4 Ω, and τ = 4 ns

current lead wire of the coaxial cable, electromagnetic field exists in the coaxial cable and does not exist around the cable. After the current arrived at the lightning stroke point, the current *I* is injected into the lightning stroke point and the current −*I* is reflected on the sheath of the coaxial cable. This current represents the return stroke propagating from the wind turbine generation system to the cloud. In the case of the measurements for winter lightning, the return stroke propagates from the cloud to the wind turbine generation system. Here, the current is injected into the coaxial cable from the pulse generator and is led to a position at a height of 6.5 m above the lightning-stroke point. At the end of the coaxial cable, the current is injected into the insulated copper wire through the resistance R_i. The lower end of the insulated copper wire is connected to the lightning-stroke point. After the current arrived at the end of the coaxial cable, the current

I is injected into the insulated copper wire. This current represents the return stroke propagating from the cloud to the wind turbine generation system. The fast-front current generated by the pulse generator is injected using a 480-Ω resistor R_i from a current lead wire in the case of summer lightning and using a 4-kΩ resistor in the case of winter lightning. The internal resistance of the pulse generator is 50 Ω, and the surge impedance of the insulated copper wire used as the current lead wire is approximately 500 Ω. Therefore, the total surge impedance of the lightning channel is (480 + 50 + 500) Ω which is approximately 1 kΩ in the case of summer lightning; on the other hand, the surge impedance becomes approximately 500 Ω, which is the surge impedance of the insulated copper wire, in the case of winter lightning. To represent the surge impedance of the lightning channel of 1 kΩ in the case of winter lightning, the insulated copper wire

becomes very thin. Therefore, the usual insulated copper wire was used in this experiment. The current lead wire and the voltage measuring wire are orthogonalized, as shown in Fig. 2, to decrease the mutual electromagnetic induction. A resistor R_g (0 Ω, 9.4 Ω, or 20 Ω), which represents the grounding resistance, is inserted between the tower foot and the aluminum plate. The wave front τ of the injected current is varied as 4 ns, 10 ns, 20 ns, or 60 ns.

III. ANALYTICAL CONDITIONS

The measurements introduced in chapter 2 are reproduced by using the electromagnetic field analysis of the FDTD method. The FDTD analytical spaces are shown in Fig. 3. The dimensions of the analytical space are 6 m × 5 m × 7.5 m and it is divided into cube cells with a side length of 2.5 cm. The absorbing boundary condition is 2nd order Liao. A thin-wire model to model the current lead wire, voltage measuring wire, and lightning conductor on a blade is used [5]. The nacelle is a cubic conductor with a side length of 15 cm, and the tower is a tube conductor with a stair-like surface. The lumped resistance representing the grounding resistance R_g is inserted between the tower foot and the aluminum plate. The current source paralleled with the resistance R_i is connected exactly above the lightning-stroke point in the case of the summer lightning. In the case of the winter lightning, it is connected at a height of 6.5 m above the lightning-stroke point.

## IV. LIGHTNING SURGE PROPAGATION ON A WIND TURBINE GENERATION SYSTEM

In Figs. 4 to 7, the injected current I and the potential V at the stroke points are shown. These values are normalized to 1 A for the peak value of the net injected current.

Figs. 4 to 7 (b) show the voltages at the stroke points. The solid line indicates the measured results and the broken line indicates the calculated results. The voltage waveform in Figs. 4 and 6 can be explained as follows: when current is injected at the tip of the blade equipped with the parallel lightning conductor, the current propagates along the lightning conductor. During this process, the intensity of the electric and magnetic fields generated around the lightning conductor increases, resulting in an increase in the voltage at the tip of the blade. After the traveling wave reaches the nacelle, the surge impedance of the nacelle becomes smaller than that of the lightning conductor; therefore, a negative reflection is caused at the nacelle, and the negative traveling wave returns to the tip of the blade. The electric and magnetic fields around the blade start weakening; further, the voltage at the tip attains its peak value when the negative reflected wave reaches the tip again. Since the return propagation time of the blade is 5 ns, the peak of the voltage appears after approximately 5 ns. The second peak of the voltage at approximately 17 ns is mainly influenced by the surge impedance of the tower, and the traveling waves on the lightning conductors that have an open end are superimposed on the voltage. Meanwhile, the voltage waveforms in Figs. 5 and 7 can be explained as follows: as

soon as current is injected into the rear portion of the nacelle, the traveling wave disperses to the three blades and the tower. Because these surge impedances are connected in parallel, the voltage rise is small for 5 ns. After 5 ns, the positive traveling waves return to the nacelle from the tips of the blades, and the voltage at the rear portion of the nacelle starts increasing because of the current flow through the tower. The voltage rise exhibits a peak when the negative traveling wave at the tower foot reaches the nacelle (after approximately 11 ns).

In both winter and summer lightning, the shapes of the voltage curves are almost the same, as shown in Figs. 4 to 7. However, the magnitudes in both these conditions are different because a part of the traveling wave from above is reflected to the upper current lead wire, while a part of it permeates through the wind turbine generation system in the case of winter lightning.

The results calculated using FDTD for R_g = 0 Ω, 9.4 Ω, and
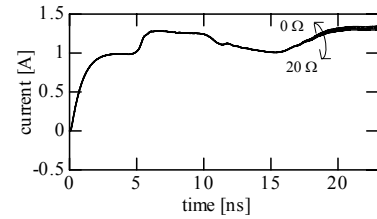
(a) Current I from FDTD analytical results
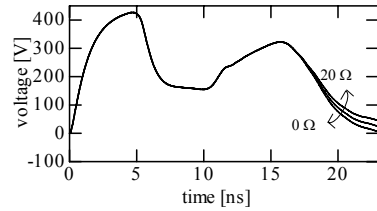
(b) Voltage V from FDTD analytical results

Fig. 8. Relations between V, I, and R_g under the conditions of summer lightning, top of the blade and $\tau = 4$ ns
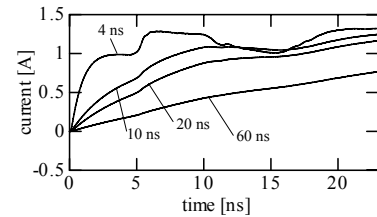

(a) Current I from FDTD analytical results
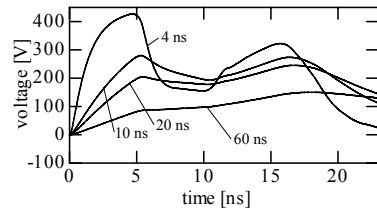

(b) Voltage V from FDTD analytical results

Fig. 9. Relations between V, I, and τ under the conditions of summer lightning, top of the blade, and R_g = 9.4 Ω

20 Ω are shown in Fig. 8. The voltage waveforms obtained for R_g = 0 Ω, 9.4 Ω, and 20 Ω change after approximately 17 ns because the reflected wave at the tower foot is different in each condition. The calculated results for τ = 4 ns, 10 ns, 20 ns, and 60 ns are shown in Fig. 9. In the case of summer lightning at the top of the blade, the second peak of V becomes larger than its first peak when the wavefront of the injected current becomes large.

V. OVERVOLTAGE CAUSED BY POTENTIAL RISE

V_{11} to V_{14} in Fig. 10 represent the voltage differences between the tower foot and the incoming conductor directed from a distant point and grounded at the remote end; depending on the grounding resistance, this voltage difference is caused by the voltage increase at the tower foot. In particular, the voltage difference becomes an overvoltage between the power line and the power converter or transformer on the ground level installed inside the tower or that between a communication line and a telecommunication device. The incoming conductor is an insulated copper wire or coaxial cable traced on the aluminum plate from a distant point and grounded at the remote end. The length of the conductors is 4.5 m. The large earth capacitance of the traced conductor is comparable to that of the underground cables in actual wind turbine generation systems.

The measured and calculated results are shown in Fig. 11 under the conditions of summer lightning, top of the blade, R_g = 9.4 Ω, and τ = 4 ns. In the FDTD analyses, it is difficult to model a coaxial cable because a side of the cube cells that is part of the FDTD space is not sufficiently larger than the radius of the coaxial cable. In this FDTD analyses, only V_{11} is calculated. V_{11} to V_{13} become nearly identical to the waveform shown in Fig. 11. The same tendency is observed in the other conditions. The potential of the insulated copper wire and the metal sheath of the coaxial cable become nearly equal because they are connected to the aluminum plate at the remote end. Therefore, there is no large difference between V_{11} and V_{12}. The potential of the core of the coaxial cable becomes nearly equal to that of the metal sheath that covers the core. Therefore, the difference between V_{12} and V_{13} is not significant. In order to suppress the overvoltage between the incoming
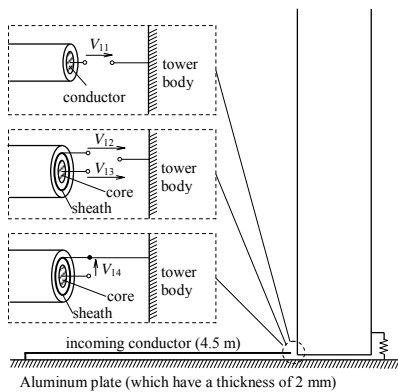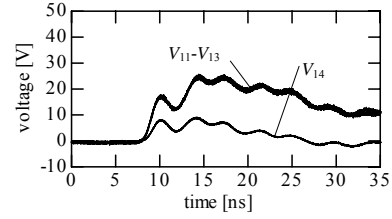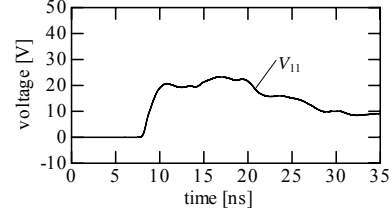

(a) Voltage V_{11}–V_{14} of measured results

(b) Voltage V_{11} of FDTD analytical results
Fig. 11.   Potential differences between the incoming conductor and the tower foot under the conditions of summer lightning, top of the blade, R_g = 9.4 Ω and τ = 4 ns)

conductor and the tower foot, the metal sheath of the coaxial cable is connected to the ground of the tower foot. The voltage difference V_{14} in such case is suppressed, 40–80%, as compared with V_{13}.

The relations between the maximum value of V_{11} to V_{13} and τ under the conditions R_g = 0 Ω, 9.4 Ω, and 20 Ω are shown in Fig. 12. The relations between the maximum values of V_{11} to V_{13} and R_g under the conditions τ = 4 ns, 10 ns, 20 ns, and 60 ns are shown in Fig. 13. The maximum value of V_{11} to V_{13} decreases with an increase in τ and is proportional to R_g. Moreover, in the case of R_g = 0 Ω, the maximum value of V_{11} to V_{13} becomes 12 V/A, which is caused by the electromagnetic induction from the current following through the tower and aluminum plates.

The same tendency is observed in the relations between the maximum value of V_{14} and τ and that between the maximum value of V_{14} and R_g. In the case of R_g = 0 Ω, the maximum value of V_{14} becomes 5.9 V/A.

VI. CONCLUSIONS

In this paper, we have presented the results of experimental and analytical studies undertaken for the lightning protection of wind turbine generation systems. This study focuses on the overvoltages observed at the wavefronts of lightning surges. Based on the investigations, the voltage rise due to the tower grounding resistance can result in a voltage difference between the tower foot and an incoming conductor directed from a distant point. The traveling-wave phenomena in the wind turbine generation system, in which lightning strikes the tip of a blade and the nacelle in summer and winter lightning, have been clarified on the basis of the measured waveforms. The above phenomena have been confirmed by using the FDTD method.

In the future, these results will be compared with the troubles in the actual wind turbine generation systems, and we try to find the cause of the troubles.
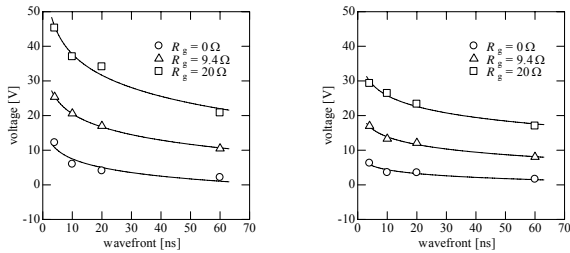
Fig. 10.   Overvoltage caused by voltage rise of the tower foot

(a) Case of the summer lightning and strike at the top of the blade (left figure)
(b) Case of the summer lightning and strike at the rear portion of the nacelle (right figure)
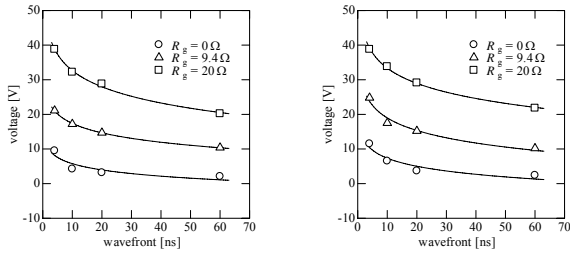
(c) Case of the winter lightning and strike at the top of the blade (left figure)
(d) Case of the winter lightning and strike at the rear portion of the nacelle (right figure)
Fig. 12.   Relations between the maximum values of V_{11} to V_{13} and τ
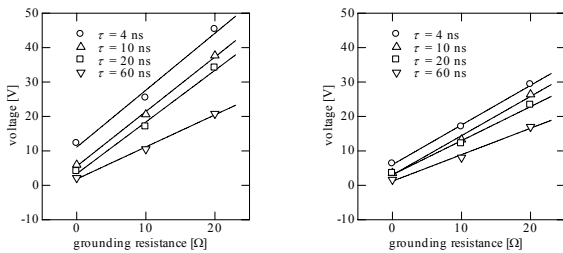

(a) Case of the summer lightning and strike at the top of the blade (left figure)
(b) Case of the summer lightning and strike at the rear portion of the nacelle (right figure)
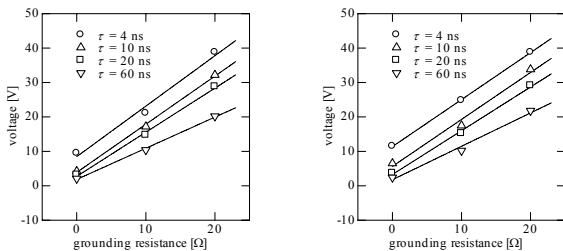

(c) Case of the winter lightning and strike at the top of the blade (left figure)
(d) Case of the winter lightning and strike at the rear portion of the nacelle (right figure)
Fig. 13.   Relations between the maximum values of V_{11} to V_{13} and R_g

VII. ACKNOWLEDGMENT

VIII. REFERENCES

[1] I. Cotton, B. Mcniff, T. Soerenson, W. Zischank, P. Christiansen, M. Hoppe-Kilpper, S. Ramakers, P. Pettersson, and E. Muljadi, "Lightning Protection for Wind Turbines," in *Proc. 25th International Conference on Lightning Protection*, pp. 848-853, Rhodes, Greece, September 2000.

[2] IEC TR 61400-24, Wind Turbine Generator Systems-Part 24: Lightning protection, 2002.

[3] K. Yamamoto, T. Noda, S. Yokoyama, A. Ametani, "An Experimental Study of Lightning Overvoltages in Wind Turbine Generation Systems Using a Reduced-Size Model," *Trans. of IEEJ*, vol. 126-B, No. 1, pp. 65–72, January 2006 (in Japanese).

[4] K. S. Kunz and R. J. Luebbers, *The Finite Difference Time Domain Method for Electromagnetics*, Boca Raton, Fl: CRC, 1993.

[5] T. Noda and S. Yokoyama, "Thin wire representation in finite difference time domain surge simulation," *IEEE Trans. Power Delivery*, vol. 17, pp. 840–847, July 2002.

Kazuo Yamamoto (M'99) was born in Osaka, Japan in 1974. He received his Bachelor's and Master's degrees in engineering from Doshisha University, Kyoto, Japan in 1997 and 2000 respectively.

He had been with Nara National College of Technology from 2000 to 2005. He has been an assistant professor at Kobe City College of Technology since 2006. From 1998 to 1999 he was a Visiting Researcher at the Manitoba HVDC Research Centre, Winnipeg, Manitoba, Canada. His research interest includes lightning protection.

Taku Noda (M'97) was born in Osaka, Japan in 1969. He received his Bachelor's, Master's, and Doctoral degrees all in engineering from Doshisha University, Kyoto, Japan in 1992, 1994, and 1997 respectively.

In 1997 he joined Central Research Institute of Electric Power Industry (CRIEPI). He is currently a Research Scientist there. From 2001 to 2002 he was a Visiting Scientist at the University of Toronto, Toronto, Ontario, Canada. From 2005 he has been serving also as an Adjunct Professor at Doshisha University. His research interest includes electromagnetic transient analysis of power systems and analysis of surges using electromagnetic field computations.

Shigeru Yokoyama (M'83, SM'91, F'96) was born in Miyagi, Japan on March 5, 1947. He received his bachelor's and PhD degrees in engineering from the University of Tokyo, Tokyo, Japan in 1969 and 1986 respectively.

In 1969, he joined CRIEPI, where he is currently an Executive Research Scientist. He is also a Visiting Professor at Kyushu University, Fukuoka, Japan. His primary research interest is the lightning protection and insulation co-ordination of transmission and distribution lines. Dr. Yokoyama is a member of IEE of Japan.

Akihiro Ametani (M'71-SM'83-F'92) was born in Nagasaki, Japan on February 14, 1944. He received B.Sc. and M.Sc. Degrees from Doshisha University in 1966 and 1968 respectively and Ph.D. degree from University of Manchester in 1973.

He had been with Doshisha University from 1968 to 1971, the University of Manchester Institute of Science and Technology from 1971 to 1974, and Bonneville Power Administration for summers from 1976 to 1981. He has been a professor at Doshisha University since 1985. He had been the Director of the Institute of Science and Engineering from 1997 to 1998, and Dean of Library and Computer/Information Center in the same university from 1998 to 2001. Dr. Ametani is a Chartered Engineer in U.K., a Distinguished Member of CIGRE and a Fellow of the IEE and was a vice-president of IEE of Japan.